



1st International Conference on Energy and Power, ICEP2016, 14-16 December 2016, RMIT University, Melbourne, Australia

## Growth of hydrogenated nano-crystalline silicon (nc-Si:H) films by plasma enhanced chemical vapor deposition (PE-CVD)

Ashok Jadhavar<sup>a</sup>, Amit Pawbake<sup>a</sup>, Ravindra Waykar<sup>a</sup>, Vijaya Jadkar<sup>a</sup>, Rupali Kulkarni<sup>a</sup>, Ajinkya Bhorde<sup>a</sup>, Sachin Rondiya<sup>a</sup>, Adinath Funde<sup>a</sup>, Dinkar Patil<sup>b</sup>, Abhijit Date<sup>c</sup>, Habib Pathan<sup>d</sup>, Sandesh Jadkar<sup>d,\*</sup>

<sup>a</sup>School of Energy Studies, Savitribai Phule Pune University, Pune 411 007, India

<sup>b</sup>Department of Metallurgical Engineering and Materials Science, IIT Powai, Mumbai 400 076, India

<sup>c</sup>School of Engineering, RMIT University, Melbourne 3000, Australia

<sup>d</sup>Department of Physics, Savitribai Phule Pune University, Pune 411 007, India

### Abstract

Hydrogenated nanocrystalline silicon (nc-Si:H) thin films were prepared by home-made PE-CVD system from gas mixture of pure SiH<sub>4</sub> and H<sub>2</sub> at various deposition pressures. Obtained results exhibited that deposition rate increases with increase in deposition pressure. Raman spectroscopy analysis revealed that deposition pressure in PE-CVD is a critical process parameter to induce nanocrystallization in Si:H films. The FTIR spectroscopy analysis results indicate that with increase in deposition pressure hydrogen bonding in films shifts from Si-H to Si-H<sub>2</sub> and (Si-H<sub>2</sub>)<sub>n</sub> bonded species bonded species. The bonded hydrogen content didn't show particular trend with optical band gap with change in deposition pressure. The obtained results indicates that 400 mTorr is an optimized deposition pressure of our PE-CVD unit to synthesize nc-Si:H films. At this optimized deposition pressure nc-Si:H films with crystallite size ~ 5.43 nm having good degree of crystallinity (~77 %) and high band gap (E<sub>Tauc</sub> ~ 1.85 eV) were obtained with a low hydrogen content (4.28 at. %) at moderately high deposition rate (0.75 nm/s). The ease of the present work is to optimize deposition pressure to obtain device quality intrinsic nc-Si:H layer in view of its used in p-i-n solar cells.

© 2017 The Authors. Published by Elsevier Ltd. This is an open access article under the CC BY-NC-ND license (<http://creativecommons.org/licenses/by-nc-nd/4.0/>).

Peer-review under responsibility of the organizing committee of the 1st International Conference on Energy and Power.

**Keywords:** PECVD; nc-SiH; Raman spectroscopy; FTIR spectroscopy

\* Corresponding author. Tel.: +91 20 2569 5201; fax: +91 20 2569 5201.  
E-mail address: sandesh@physics.unipune.ac.in

## 1. Introduction

Hydrogenated nano-crystalline silicon (nc-Si:H) has been the subject of scientific and technological interest in recent years because of its outstanding properties such as tailorable band gap [1], high intrinsic conductivity [2], higher carrier mobility [3], higher doping efficiency [4] and high stability [5] against the prolonged light illumination in comparison to a-Si:H. With the perspective of increase in the conversion efficiency of thin film solar cells, use of nc-Si:H in a-Si based solar cells has been suggested, and much progress regarding the preparation and performance of nc-Si:H material and solar cells has been made in the past few years. A variety of deposition techniques have been used for the preparation of nc-Si:H to yield material with good opto-electronic properties. Several chemical vapor deposition techniques such as plasma enhanced CVD (PE-CVD) [6] and its variant, electron cyclotron resonance CVD [7] and hot wire CVD (HW-CVD) [8] very high frequency plasma enhanced chemical vapor deposition (VHF-PECVD) [9] and microwave CVD [10]. Some other methods also already tried which includes magnetron sputtering [11], layer by layer deposition [12], etc. Out of these, only PE-CVD have been successfully used for the preparation of nc-Si:H films with device quality films. In the preparation of nc-Si:H by PE-CVD, usually high hydrogen dilution of silane and high RF power are used. The use of high hydrogen dilution of silane resulted in lower deposition rate while use of high RF power resulted in improvement of electrical conductivity of nc-Si:H layer but degradation of transparent conducting coating on which solar cells is fabricated. For industrial applications, high deposition rates with good opto-electrical properties are required. Therefore, preparation of nc-Si:H films at high deposition rates while maintaining good material quality is of major technological importance.

It is generally believed that the properties of nc-Si:H films prepared by PE-CVD are strongly affected by the process parameters such as substrate temperature, process pressure, inter-electrode distance, RF power, hydrogen dilution of source gases etc. These studies are based on the understanding the influence of only one of these process parameters on nc-Si:H films. However, there is lot of room for the improvement of film properties since the relation between the variation of deposition parameter and the resulting film properties has not been fully elucidated yet. It is with this motivation that we initiated the detailed study of synthesis and characterization of intrinsic nc-Si:H films using PE-CVD method. In this paper, we present detail investigation of influence of deposition pressure on structural, optical, and electrical properties of nc-Si:H films deposited by PE-CVD method. Obtained results exhibited that these properties critically depends on deposition pressure.

## 2. Experimental

### 2.1. Film preparation

Intrinsic hydrogenated nanocrystalline silicon (nc-Si:H) thin films were deposited simultaneously on corning #7059 glass and c-Si wafers by indigenously designed and locally fabricated plasma enhanced chemical vapor deposition (PE-CVD) unit, schematic of which is shown in Fig. 1.

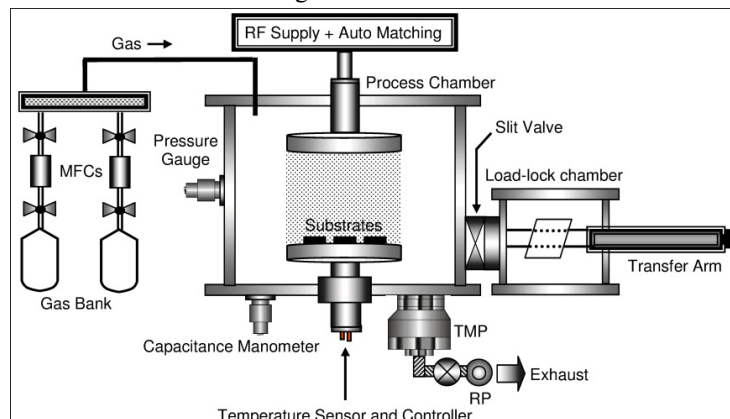


Fig. 1. Schematic diagram of indigenously designed and locally fabricated plasma enhanced chemical vapor deposition (PE-CVD).

Films were prepared by using pure silane ( $\text{SiH}_4$ ) as Si source gas and hydrogen ( $\text{H}_2$ ) as dilution gas. The flow rate of  $\text{SiH}_4$  and  $\text{H}_2$  are kept constant at 1.5 sccm and 100 sccm respectively. The substrate temperature was held constant during the deposition. Other deposition parameters are listed in Table 1.

Table 1. Process parameters used of the deposition of intrinsic nc-Si:H thin films by PE-CVD method.

Process parameter	Value
Deposition temperature ( $T_{\text{Sub}}$ )	400 °C
Distance between electrodes (d)	3 cm
Silane flow rate ( $F_{\text{SiH}_4}$ )	1.5 sccm
Hydrogen flow rate ( $F_{\text{H}_2}$ )	100 sccm
Deposition pressure ( $P_d$ )	100-700 mTorr
RF Power (P)	60Watt
Deposition Time (t)	30 min

The glass substrates were cleaned with double distilled water whereas, the c-Si wafers were given an HF etch to remove native oxide layer. The substrates were loaded to the substrate holder and then the deposition chamber was evacuated to the base pressure less than  $10^{-6}$  Torr. Prior to each deposition, the substrate holder and deposition chamber were baked for two hours at 100 °C to remove any water vapor absorbed on the substrates and to reduce the oxygen contamination in the film. After that, the substrate temperature was brought to desired value by appropriately setting the inbuilt thermocouple and temperature controller. The deposition was carried out for desired amount of time and films were allowed to cool to room temperature in vacuum.

## 2.2. Film characterization

Raman spectra were recorded with Raman spectroscopy (Renishaw InVia Confocal Raman Microscope) in the wave number range  $100\text{-}1000\text{ cm}^{-1}$ . The spectrometer has backscattering geometry for detection of Raman spectrum with the resolution of  $1\text{ cm}^{-1}$ . The power of the Raman laser was kept less than 10 mW to avoid laser induced crystallization on the films. Deposited films have been studied for their optical properties by UV-Vis-NIR Spectroscopy (JASCO, V-670). The optical absorption coefficient ( $\alpha$ ) was determined from the transmission (% T) and reflection (% R) measurements. The band gap was estimated using the procedure followed by *Tauc* [13]. The FTIR spectra were recorded in transmission mode by using FTIR spectrophotometer (JASCO, 6100-type A). Bonded hydrogen content ( $C_H$ ) was calculated from wagging mode of FTIR absorption peak using the method given by the *Brodsky et al.* [14]. Dark conductivity ( $\sigma_{\text{dark}}$ ) and photoconductivity ( $\sigma_{\text{photo}}$ ) were measured using samples of dimension 3 cm x1 cm deposited on glass substrate with coplanar Al electrodes 0.5 mm apart deposited by vacuum evaporation. Thickness of films was determined by profilometer (KLA Tencor, P-16+) and was further confirmed by UV-Visible spectroscopy using the method proposed by *Swanepoel* [15].

## 3. Results and discussion

### 3.1. Variation of film deposition rate

Fig. 2 shows the relation between the deposition rate and deposition pressure. As seen from the figure the highest deposition rate is obtained for the film deposited at  $P_d = 400$  mTorr and it decreases at low as well as high deposition pressure. At low deposition pressure ( $< 400$  mTorr) it is expected that the primary film forming radicals directly reach the substrate surface without any gas phase reactions and results increase in deposition rate. However, as deposition pressure becomes higher ( $> 400$  mTorr) the gas transport shifts from molecular to viscous due to collisions in the gas phase. Therefore, the supply of film forming radicals to substrate surface becomes restricted and consequently the deposition rate decreases at higher deposition pressure. Furthermore, at higher deposition pressure the collisions between the primary generated radicals and ambient  $\text{SiH}_4$  and  $\text{H}_2$  will also occur. This leads to the formation of lower sticking coefficient species, resulting in a reduction of the deposition rate at higher deposition pressure.

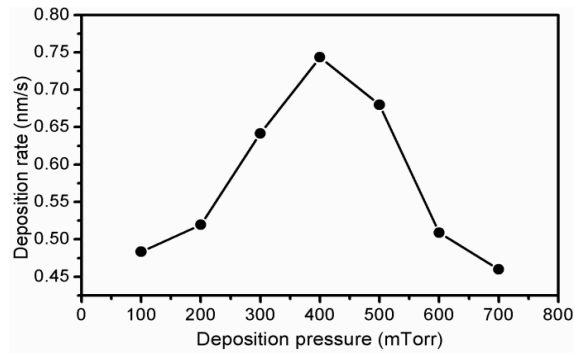


Fig. 2. Variation of deposition rate as a function of deposition pressure for Si:H films deposited by PE-CVD.

### 3.2. Raman spectroscopy analysis

Raman spectroscopy is a non-destructive tool of analysis which provides direct structural information quantitatively related to the average crystallite size and the crystalline volume fraction in the film. Fig. 3(a) shows the Raman spectra of Si:H films deposited at various deposition pressures ( $P_d$ ).

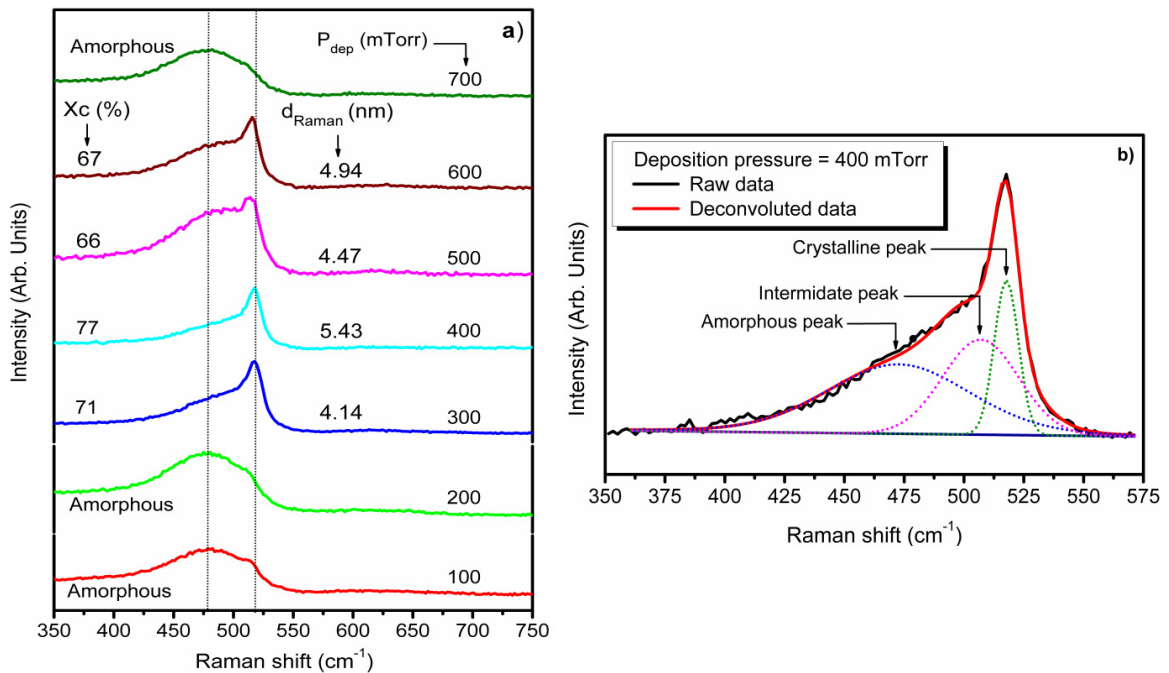


Fig. 3. a) Raman spectra of Si:H films deposited at various deposition pressures by PE-CVD method b) Typical de-convoluted Raman spectra for the film deposited at  $P_d = 400$  mTorr.

To estimate the volume fraction of crystallites and crystallite size, each spectrum in figure 3 was de-convoluted into three peaks with a quadratic base line using Levenberg-Marquardt method [16], a crystalline peak ( $\sim 520$   $\text{cm}^{-1}$ ), an amorphous peak ( $\sim 480$   $\text{cm}^{-1}$ ) and an intermediate peak, ( $\sim 510$   $\text{cm}^{-1}$ ). Typical de-convoluted Raman spectra for Si:H film deposited at  $P_d = 400$  mTorr is shown in Fig. 3(b). Crystalline fraction ( $X_{Raman}$ ) was calculated using  $X_{Raman} = I_c + I_m / (I_c + I_m + I_a)$  [17], where  $I_c$  is the integrated intensity of the crystalline phase near  $520$   $\text{cm}^{-1}$ ,  $I_m$  is the integrated intensity of the intermediate phase around  $500$   $\text{cm}^{-1}$  and  $I_a$  is the integrated intensity of the amorphous phase at  $480$   $\text{cm}^{-1}$ . The crystallite size ( $d_{Raman}$ ) was deduced using  $d_{Raman} = 2\pi(\beta/\Delta\omega)^{1/2}$ , where  $\Delta\omega$  is the peak shift compared to c-Si peak located  $\sim 520$   $\text{cm}^{-1}$  and  $\beta = 2.0$   $\text{cm}^{-1}\text{nm}^2$  [18]. As seen from figure 4(a) films deposited at low  $P_d$  ( $> 200$

mTorr) show only a broad shoulder centered  $\sim 480 \text{ cm}^{-1}$  which corresponds to typical a-Si:H material. However, the film deposited at  $P_d = 300 \text{ mTorr}$ , shows the onset of nanocrystallization. Raman spectra for this film show a broad shoulder centered  $\sim 480 \text{ cm}^{-1}$ , associated with the amorphous and the other transverse optic (TO) phonon peak centered  $\sim 518 \text{ cm}^{-1}$  originating from nanocrystalline phase [19]. For this film,  $X_{\text{Raman}}$  is  $\sim 71 \%$  and  $d_{\text{Raman}}$  is  $\sim 4.14 \text{ nm}$ . This clearly indicates that with increase in deposition pressure results in an amorphous-to-nanocrystalline transition in the film. Further increase in  $P_d$ , the peak shift towards lower wave number indicating decrease in volume fraction of crystallites. As a result, the film deposited at  $P_d = 600 \text{ mTorr}$ , the Raman spectra shows nanocrystalline phase with the TO phonon peak centered  $\sim 515 \text{ cm}^{-1}$  and a small amorphous content in it. For this film,  $X_{\text{Raman}}$  is  $\sim 67 \%$  and  $d_{\text{Raman}}$  is  $\sim 4.94 \text{ nm}$ . The Raman spectra for the film deposited at  $P_d = 700 \text{ mTorr}$  the TO peak associated nanocrystalline phase disappear completely and a broad shoulder associated with amorphous phase emerged at  $\sim 480 \text{ cm}^{-1}$  suggesting amorphization of the film. Thus, it is concluded that deposition pressure in PE-CVD is a critical process parameter to induce nanocrystallization in Si:H films.

### 3.3. Fourier transform Infra-red (FTIR) spectroscopy analysis

The FTIR spectra of nc-Si:H films (at normalized thickness) deposited by PE-CVD method at different deposition pressure are shown in Fig. 4(a). For clarity, the spectra have been broken horizontally into two parts.

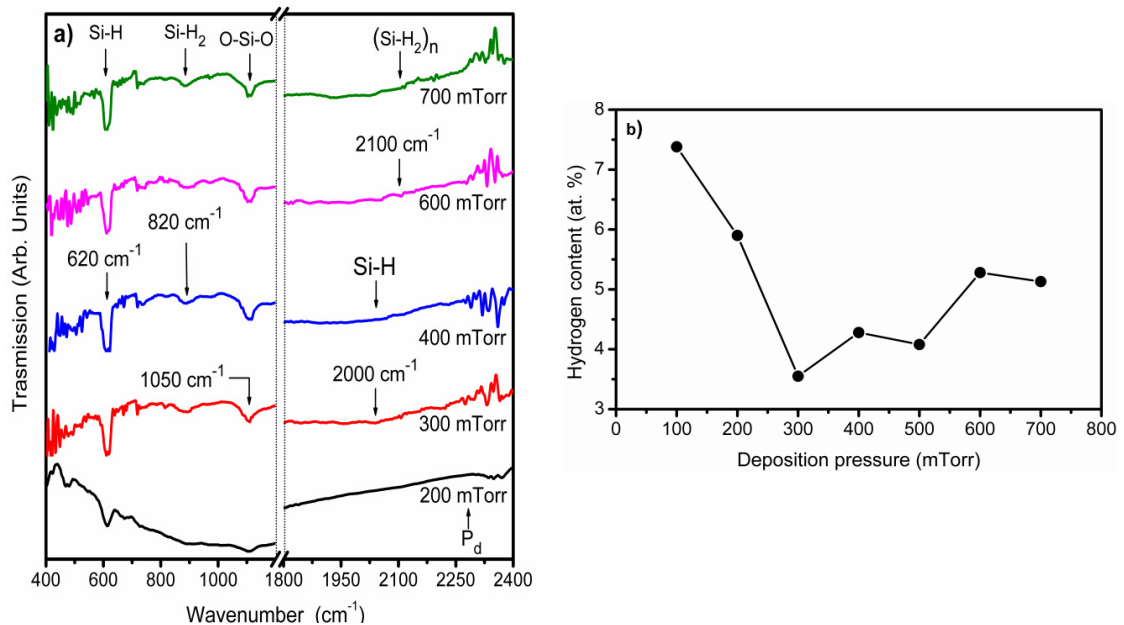


Fig. 4. a) FTIR spectra and b) Variation of hydrogen content as a function of deposition pressure for nc-Si:H films deposited by PE-CVD.

It can be seen from the spectra that all films have two major absorption bands centered at  $\sim 620 \text{ cm}^{-1}$  and  $\sim 2000 \text{ cm}^{-1}$  corresponding to the wagging/stretching modes, respectively, of vibrations of mono-hydrogen (Si-H) bonded species [20]. The spectra also exhibit two absorption peaks one centered  $\sim 1050 \text{ cm}^{-1}$  and other less intense centered  $\sim 885 \text{ cm}^{-1}$ . The absorption peaks centered  $\sim 1050 \text{ cm}^{-1}$  associated with the asymmetric Si-O-Si stretching vibrations. This is indicative of an oxidation effect caused by its porous-like microstructure, which is a typical feature for undoped nc-Si:H thin films [21]. The absorption peak centered  $\sim 885 \text{ cm}^{-1}$  can be assigned to the bending vibrational modes of Si-H<sub>2</sub> and (Si-H<sub>2</sub>)<sub>n</sub> complexes [22]. These results indicate that the hydrogen in the films predominantly incorporated in mono-hydrogen (Si-H) species. With increase in deposition pressure the intensity of absorption band at  $\sim 620 \text{ cm}^{-1}$  increases and an absorption band centered  $\sim 2100 \text{ cm}^{-1}$  emerged out which can be assigned to stretching vibrational modes of di-hydride, Si-H<sub>2</sub> and poly-hydride, (Si-H<sub>2</sub>)<sub>n</sub> bonded species (isolated or coupled) respectively [23]. These

results indicate that with increase in deposition pressure the predominant hydrogen bonding in films shifts from Si-H to Si-H<sub>2</sub> and (Si-H<sub>2</sub>)<sub>n</sub> bonded species bonded species.

Fig. 4(b) shows the variation of hydrogen content ( $C_H$ ) as a function of deposition pressure. As seen from the figure, hydrogen content first decreases with increase in deposition pressure from 100 to 300 mTorr and then it increases gradually with further increase in deposition pressure to 700 mTorr. It is interesting to note that the hydrogen content was found less than 8 at. % over the entire range of deposition pressure studied. As seen from the FTIR spectra (Fig. 5) at low deposition pressures the the hydrogen in the films predominantly incorporated in mono-hydrogen (Si-H) species as a result bounded hydeogen content in the is less. However, at high deposition pressures increase in hydrogen content may attributed to the formation of defects or disorders or voids due to the amorphization of films as revealed from Raman spectroscopy analysis (Fig. 3). The grain boundaries of defects and voids seem to be passivated by large amount of hydrides, silicon-hydrogen bonds suggesting increase of hydrogen content in the films at higher deposition pressures.

### 3.4. UV-Visible spectroscopy analysis

Optical properties nc-Si:H films were deduced from transmission (T) and reflection (R) spectra using UV-Visible spectrophotometer. In the direct transition semiconductor, band gap ( $E_{Tauc}$ ) and absorption coefficient ( $\alpha$ ) are related by  $(\alpha E)^{1/2} = B^{1/2} (E - E_{Tauc})$  [14], B is the optical density of state and E is the photon energy. The absorption coefficient ( $\alpha$ ) can be calculated with the formula  $\alpha = 1/d \ln (1/T-R)$  [24], where d is thickness of the films. Therefore, optical band gap is obtained by extrapolating tangential line to photon energy ( $E = h\nu$ ) axis in the plot of  $(\alpha h\nu)$  versus  $h\nu$ . Fig. 5 shows variation of optical band gap as a function of deposition pressure. Band gap decreases with increase in deposition pressure. It is generally accepted that the band gap of Si:H depends on the hydrogen content and it linearly increases with the increase in hydrogen content [25]. However, in present study, no specific trend has been found between hydrogen content and band gap. Thus, the amount of bounded hydrogen only cannot account for the band gap in nc-Si:H films. We think that increase in band gap may be due to increase in defect density in the films with increase in deposition pressure. Variation of defect density as a function of deposition pressure is shown in Fig. 5. Films are more disordered in nature due to the increase in deposition rate with increase in deposition pressure. Increasing intensity of Si-O-Si stretching mode absorption band  $\sim 1050 \text{ cm}^{-1}$  [23] in FTIR spectra suggest increasing concentration of O impurity in the film with increasing deposition pressure. The excess oxidation appears to be associated with an increase in the defect density, resulting in disordered structures [26].

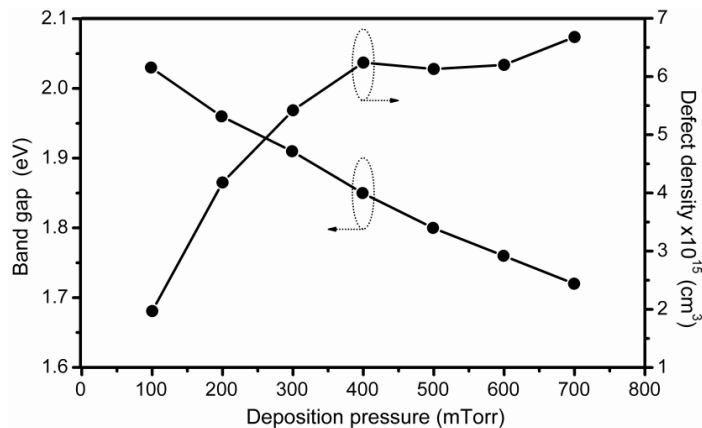


Fig. 5. Variation of optical band gap and defect density as a function of deposition pressure for nc-Si:H films deposited by PE-CVD.

### 3.5. Electrical Properties

Thin films deposited on glass substrates of dimension  $1 \text{ cm} \times 2 \text{ cm}$  were prepared and Al electrodes 0.5 mm apart were deposited by thermal evaporation and loaded to a specially designed sample holder and the contacts were

developed using Ag paste. The measurements at room temperature were carried out at atmospheric pressure. A voltage of  $\sim 60$  V DC was applied to the electrodes and the current was measured using a system electrometer (Keithley, Model 6514). The measurements were done first under dark condition, and then the specimen was illuminated by a Xe lamp, with an intensity  $100 \text{ mW/cm}^2$ , which was calibrated using a standard c-Si solar cell. The dark conductivity ( $\sigma_{\text{dark}}$ ) and photoconductivity ( $\sigma_{\text{photo}}$ ) were calculated using relation  $\sigma = [(V \times d \times \omega)/(I \times l)]^{-1}$ , where V is applied voltage, I is current, d is thickness,  $\omega$  is width and l is the distance between electrodes. Table 2 shows obtained values of dark and photoconductivity for nc-Si:H films deposited at different deposition pressures.

Table 2. Dark conductivity and photoconductivity for nc-Si:H films deposited at different deposition pressures.

Deposition pressure (mTorr)	Dark Conductivity (S/cm)	Photoconductivity (S/cm)
100	$9.20 \times 10^{-4}$	$1.49 \times 10^{-4}$
200	$3.64 \times 10^{-6}$	$2.61 \times 10^{-6}$
300	$2.03 \times 10^{-6}$	$1.53 \times 10^{-6}$
400	$1.56 \times 10^{-3}$	$2.99 \times 10^{-3}$
500	$8.24 \times 10^{-5}$	$9.04 \times 10^{-4}$
600	$8.69 \times 10^{-4}$	$5.00 \times 10^{-4}$
700	$1.56 \times 10^{-5}$	$5.17 \times 10^{-5}$

As seen from the table 2, both,  $\sigma_{\text{dark}}$  and  $\sigma_{\text{photo}}$  were found in the range  $\sim 10^{-3}$ - $10^{-6}$  S/cm over the entire range of deposition pressure investigated. As a result, photo-response, taken as the ratio of photoconductivity-to-dark conductivity ( $\sigma_{\text{photo}}/\sigma_{\text{Dark}}$ ) was found in the range 10 and 1. We attribute change in the photo-response to change in crystalline fraction in the film with increase in deposition pressure because the  $\mu\text{-Si:H/nc-Si:H}$  films prepared by different methods show high dark conductivity and negligible photo-response depending upon the crystallite size and its volume fraction [27]. This inference is further strengthened from Raman spectroscopy analysis.

#### 4. Conclusion

Hydrogenated nanocrystalline silicon (nc-Si:H) thin films were prepared by home-made plasma enhanced chemical vapor deposition (PE-CVD) system. We investigated the effect of deposition pressure on the structural, optical and electrical properties of nc-Si:H films by using various characterization techniques. The obtained results exhibited that the deposition rate increases with increase in deposition pressure. Raman spectroscopy analysis revealed that the deposition pressure in PE-CVD is a critical process parameter to induce nanocrystallization in Si:H films. The FTIR spectroscopy analysis results indicate that with increase in deposition pressure the predominant hydrogen bonding in films shifts from Si-H to Si-H<sub>2</sub> and (Si-H<sub>2</sub>)<sub>n</sub> bonded species bonded species. However, the bonded hydrogen content didn't show particular trend with optical band gap with change in deposition pressure. The obtained results indicates that 400 mTorr is an optimized deposition pressure of our PE-CVD unit to synthesize nc-Si:H films. At this optimized deposition pressure nc-Si:H films with crystallite size  $\sim 5.43$  nm having good degree of crystallinity ( $\sim 77$  %) and high band gap ( $E_{\text{Tauc}} \sim 1.85$  eV) were obtained with a low hydrogen content (4.28 at. %) at moderately high deposition rate (0.75 nm/s). Further detailed experiments are required to study effect of other process parameters to optimize the nc-Si:H films before starting n-and p-type doping for solar cells applications.

#### Acknowledgement

Authors are thankful to Department of Science and Technology (DST), Ministry of New and Renewable Energy (MNRE), Government of India for the financial support. Mr. Sachin Rondiya is grateful to Dr. Babasaheb Ambedkar Research and Training Institute (BARTI), Pune for research fellowship and financial assistance. Mr. Ashok Jadhavar is thankful to BARC-SPPU program for financial support. One of the authors Dr. Sandesh Jadhkar is thankful to University Grants Commission, New Delhi for special financial support under UPE program.



## References

- [1] Kitao J, Harada H, Yoshida N, Kasuya Y, Nishio M, Sakamoto T, Itoh T, Nonomura S, Nitta S. Absorption coefficient spectra of  $\mu\text{-Si}$  in the low-energy region 0.4-1.2 eV. *Sol Energ Mat Sol Cells* 2001;66: 245-251.
- [2] Ito M, Koch C, Svrcek V, Schubert M, Werne J. Silicon thin film solar cells deposited under 80°C. *Thin Solid Films* 2001;383:129-131.
- [3] Jana M, Das D, Barua A. Role of hydrogen in controlling the growth of  $\mu\text{-Si:H}$ / $\mu\text{-Si:H}$  films from argon diluted  $\text{SiH}_4\text{SiH}_4$  plasma. *J Appl Phys* 2002;91:5442-5448.
- [4] Shah A, Meier J, Vallat-Sauvain E, Wyrtsch N, Kroll U, Droz C, Graf U. Material and solar cell research in microcrystalline. *Sol Energ Mat Sol Cells* 2003;78:469-491.
- [5] Shah A. *Thin-Film Silicon Solar Cells*. EPFL Press;2010.
- [6] Rech B, Roschek T, Müller J, Wieder S, Wagner H. Amorphous and microcrystalline silicon solar cells prepared at high deposition rates using RF (13.56 MHz) plasma excitation frequencies. *Sol Energ Mat Sol Cells* 2001;66:267-273.
- [7] Birkholz M, Selle B, Conrad E, Lips K, Fuhs W. Evolution of structure in thin microcrystalline silicon films grown by electron-cyclotron resonance chemical vapor deposition. *J Appl Phys* 2000;88:4376-4379.
- [8] Li H, Franken RH, Stolk RL, van der Werf CHM, Schropp REI, Rath JK. Controlling the quality of nano crystalline silicon made by hot-wire chemical vapor deposition by using a reverse H<sub>2</sub> profiling technique. *J Non-Cryst Solids*. 2008;354:2087-2091.
- [9] Peng S, Wang D, Yang F, Wang Z, Ma F. Grown Low-Temperature Microcrystalline Silicon Thin Film by VHF PECVD for Thin Films Solar Cell. *J Nanomater* 2015;Article ID 327596:5 pages.
- [10] van Veen MK, van der Werf CHM, Schropp REI. Tandem solar cells deposited using hot-wire chemical vapor deposition. *J Non-Cryst Solids* 2004;338:655-658.
- [11] Bailey L, Proudfoot G, Mackenzie B, Andersen N, Karlsson A, Ulyashin A. High rate amorphous and crystalline silicon formation by pulsed DC magnetron sputtering deposition for photovoltaics. *Phys Status Solidi A* 2015;212:42-46.
- [12] Knoops HC, Braeken EM, de Peuter K, Potts SE, Haukka S, Pore V, Kessels WM. Atomic Layer Deposition of Silicon Nitride from Bis(tert-butylamino)silane and N<sub>2</sub> Plasma. *ACS Appl Mater Interfaces* 2015;35:19857-62.
- [13] J. Tauc. Absorption edge and internal electric fields in amorphous semiconductors. *Materials Research Bulletin* 1970;5:721-729.
- [14] Brodsky MH, Cardona M, Cuomo JJ. Infrared and Raman spectra of the silicon-hydrogen bonds in amorphous silicon prepared by glow discharge and sputtering. *Phys Rev* 1977;16:3556-3571.
- [15] Swanepoel R. Determination of the thickness and optical constants of amorphous silicon *J Phys E Sci Instrum* 1983;16:1214-1222.
- [16] Marquardt D. Algorithm for Least-Squares Estimation of Nonlinear Parameters. *J Soc Ind Appl Math* 1963;11/2:431-441.
- [17] Kaneko T, Wakagi M, Onisawa K, Minemura T. Change in crystalline morphologies of polycrystalline silicon films prepared by radio-frequency plasma-enhanced chemical vapor deposition using SiF<sub>4</sub>+H<sub>2</sub> gas mixture at 350 °C. *Appl Phys Lett* 1994;64:1865-1867.
- [18] He Y, Yin C, Cheng G, Wang L, Liu X, Hu GY. The structure and properties of nanosize crystalline silicon films. *J Appl Phys* 1994;75, 797-802.
- [19] Li Z, Li W, Jiang Y, Cai H, Gong Y, He J. Raman characterization of the structural evolution in amorphous and partially nanocrystalline hydrogenated silicon thin films prepared by PECVD. *J Raman Spectrosc*. 2011;42:415-421.
- [20] Lucovsky G. Vibrational spectroscopy of hydrogenated amorphous silicon alloys. *Solar Cells* 1980;2:431.
- [21] Halindintwali S, Knoesen D, Swanepoel R, Julies B, Arendse C, Muller T, Theron C, Gordijn A, Bronsveld P, Rath JK, Schropp REI. Improved stability of intrinsic nanocrystalline Si thin films deposited by hot-wire chemical vapour deposition technique. *Thin Solid Films* 2007;515/2:8040-8044.
- [22] Knights JC, Lucovsky G, Nemanich RJ. Defects in plasma-deposited a-Si: H. *J Non-Cryst Solids* 1979;32:393-403.
- [23] Tsu DV, Lucovsky G, Davidson BN. Effects of the nearest neighbors and the alloy matrix on SiH stretching vibrations in the amorphous SiO<sub>r</sub>:H (0<r<2) alloy system. *Phys Rev B* 1989;40:1795-1805.
- [24] Cremona A, Laguardia L, Vassallo E, Ambrosone G, Coscia U, Orsini F, Poletti G. Optical and structural properties of siliconlike films prepared by plasma-enhanced chemical-vapor deposition. *J Appl Phys* 2005;97:0235331-0235335.
- [25] Amor SB, Atyaoui M, Bousbih R, Haddadi I, Dimassi W, Ezzaouia H. Effect of substrate temperature on microstructure and optical properties of hydrogenated nanocrystalline Si thin films grown by plasma enhanced chemical vapor deposition. *Sol Energy* 2014;108:126-134.
- [26] Lucovsky G, Nemanich RJ, Knights JC. Structural interpretation of the vibrational spectra of a-Si: H alloys. *Phys Rev B* 1979;19:2064-2073.
- [27] Saitoh T, Shimada T, Migitaka M, Tarui Y. Preparation and properties of microcrystalline silicon films using photochemical vapor deposition. *J Non-Cryst Solids* 1983;59-60:715-718.